Transportation Research Part A 86 (2016) 159–176

Contents lists available at ScienceDirect

Transportation Research Part A

journal homepage: www.elsevier.com/locate/tra

A hybrid simulation-assignment modeling framework for crowd dynamics in large-scale pedestrian facilities

Ahmed Abdelghany [a,*], Khaled Abdelghany [b,1], Hani Mahmassani [c,2]

[a] College of Business, Embry-Riddle Aeronautical University, 600 S. Clyde Morris Blvd., Daytona Beach, FL 32114, United States
[b] Department of Civil and Environmental Engineering, Southern Methodist University, P.O. Box 750340, Dallas, TX 75275-0340, United States
[c] Transportation Center, Northwestern University, 215 Chambers Hall, 600 Foster St., Evanston, IL 60208, United States

ARTICLE INFO

Article history:
Received 2 December 2013
Received in revised form 6 January 2016
Accepted 22 February 2016
Available online 8 March 2016

Keywords:
Crowd dynamics
Simulation models
Networks
Cellular automata
Pedestrian flow

ABSTRACT

This paper presents a hybrid simulation-assignment modeling framework for studying crowd dynamics in large-scale pedestrian facilities. The proposed modeling framework judiciously manages the trade-off between ability to accurately capture congestion phenomena resulting from the pedestrians' collective behavior and scalability to model large facilities. We present a novel modeling framework that integrates a dynamic simulation-assignment logic with a hybrid (two-layer or bi-resolution) representation of the facility. The top layer consists of a network representation of the facility, which enables modeling the pedestrians' route planning decisions while performing their activities. The bottom layer consists of a high resolution Cellular Automata (CA) system for all open spaces, which enables modeling the pedestrians' local maneuvers and movement decisions at a high level of detail. The model is applied to simulate the crowd dynamics in the ground floor of Al-Haram Al-Sharif Mosque in the City of Mecca, Saudi Arabia during the pilgrimage season. The analysis illustrates the model's capability in accurately representing the observed congestion phenomena in the facility.

1. Introduction

Large-scale pedestrian facilities are an integral and increasingly important component of the urban built environment. Examples of these facilities include exhibit and convention halls, worshipping halls, stadia and sport arenas, transit terminals, and amusement parks, to name a few. During their peak periods, these facilities serve tens or even hundreds of thousands of pedestrians, experiencing severely congested conditions that are vulnerable to the occurrence of catastrophic accidents (Still, 2010). These accidents have brought more attention to the design and the operation management process of these facilities to ensure safe and efficient operation during both normal and extreme operating conditions. Thus, modeling tools that are capable of analyzing crowd dynamics in these facilities at a high fidelity level are critical to accomplish these tasks. These modeling tools provide a platform to depict areas of deficient capacity and unsafe movement conflicts (e.g., bottlenecks), and thus help identify ways to improve system design, and develop efficient crowd management schemes under different operational scenarios. Essential capabilities that these tools should provide include: (1) detailed depiction of the architectural blueprint of the facility considering connectivity among its spaces, entrance and egress gates, and any

* Corresponding author. Tel.: +1 (386) 226 6670.
E-mail addresses: ahmed.abdelghany@erau.edu (A. Abdelghany), khaled@lyle.smu.edu (K. Abdelghany), masmah@northwestern.edu (H. Mahmassani).
[1] Tel.: +1 (214) 768 4309; fax: +1 (214) 768 2164.
[2] Tel.: +1 847 491 2282; fax: +1 847 491 3090.

http://dx.doi.org/10.1016/j.tra.2016.02.011
0965-8564/

existing obstacles; (2) accurate representation of the crowd dynamics and associated congestion phenomena resulting from the pedestrians' movement behavior and the surrounding environment; and (3) capturing the effect of crowd control strategies that might be adopted as part of proposed crowd management schemes.

Considerable effort has been devoted to developing modeling tools that can be used to study pedestrians in crowded facilities. These tools vary in the trade-off level they provide between *fidelity*, i.e., the ability to accurately capture congestion and crowd behavioral phenomena, and *scalability* to represent large facilities with complex architecture and high pedestrian demand levels (e.g., densities of 4 persons/m^2 and above). Inadequate consideration of such trade-off could result in modeling tools that are either nominally capable of representing large-scale facilities while failing to accurately capture specific congestion phenomena that might occur in these facilities at high demand levels, or tools that are successful in representing the congestion phenomena with limited ability to scale up to large facilities (Sarmady et al., 2007; Tunasar, 2013; Duives et al., 2013). As discussed in the next section, most existing models fall in the latter category.

Applications of most existing models to large facilities with intensive demand levels have been achieved by reducing the size of the modeled area, truncating the analysis horizon, or through a combination of both (Sarmady et al., 2007; Tunasar, 2013). Unfortunately, arbitrarily reducing the size of a modeled space could limit the ability to study the impact of congestion in adjacent spaces with potential flow spillback. Furthermore, truncating the analysis horizon could preclude reaching steady-state conditions, which is essential especially for capacity estimation studies.

This research is motivated by the need for a modeling framework to study crowd dynamics in large-scale (mega) pedestrian facilities that are characterized by complex architectural design with multiple connected spaces, intricate pedestrian movement patterns, and extreme congestion. In this research the term "crowd" refers to a large number of persons that are temporarily gathered closely together; responding to common stimuli and engaged in various forms of collective behavior. The term "congestion" refers to a state of overcrowding and space that is filled with more people than is desirable. The desirable level could be defined by the crowd themselves or by the facility operators.

This research contributes to the existing literature by introducing a new modeling framework that judiciously manages the trade-off between ability to accurately capture congestion phenomena resulting from the pedestrians' collective behavior, and scalability to model large facilities. The framework integrates a dynamic simulation-assignment logic with a hybrid (two-layer or bi-resolution) representation of the facility. The top layer consists of a network representation of the facility, which enables modeling the pedestrians' route planning decisions while performing their activities. The bottom layer consists of a high resolution Cellular Automata (CA) system for all open spaces, which enables modeling the pedestrians' local maneuvers and movement decisions at a high level of detail. Accordingly, the paper contributes primarily through providing (1) hybrid, bi-resolution modeling approach and system representation, (2) ability to address both tactical-level pedestrian path choices as well as embedded operational-level behaviors in density levels that may attain extreme levels, (3) improved agent interaction mechanisms in dense crowds that provide realistic representation of observed phenomena, (4) application to actual system with very high demand levels and associated densities, and (5) validation against actual observation.

The framework is applied to estimate the capacity and other performance measures under a typical operational scenario of the core area of Al-Haram Al-Sharif Mosque complex in Makkah, Saudi Arabia, which is a uniquely challenging facility for crowd modeling applications (Sarmady et al., 2007; Tunasar, 2013). It serves millions of pilgrims who perform several rituals that require complex maneuvers under extreme congestion situations. The mosque consists of the main hall, which is surrounded by a multi-story building and another additional open area. It has a total capacity of 400,000 worshipers and is expected to increase to one million worshippers after an ongoing expansion. At the center of the main prayer hall, a cube-shaped shrine building known as "Al-Ka'aba Al-Mosharafa" is located. During the Hajj event, each of the nearly three million pilgrims has to visit the Mataf system, at least twice, to perform the "Tawaf" ritual. The Tawaf is a circumambulation process whereby pilgrims go around Al-Ka'aba a total of seven times in the counter-clockwise direction, starting from a predefined point (line that emanates along a radius from the center of Al-Ka'aba). During circumambulation, each pilgrim tries to come closer to Al-Ka'aba, in the hope of reaching and touching it, and also to avoid circumambulation in larger-radius loops. Upon finishing the Tawaf, pilgrims try to find a way out of the system, causing notorious crowd conflicts with other entering and looping pilgrims. The facility usually encounters high level of density of 8 persons/m^2, with pilgrims expect to walk at relatively lower speed with humbleness and modesty (Curtis et al., 2011). The crowd consists of a heterogeneous set of pilgrims, varying with respect to activity, walking speed, and congestion perception. All these factors make the facility unique and accordingly the results of this application should not be generalized to other facilities.

The next section provides a review of existing models with focus on simulation approaches and applications. Detailed description of the proposed modeling framework is then presented, including the bi-resolution approach used to combine network-based routing and activity implementation of pedestrians, with the complex interactions taking place in the flow systems. The formulation of the models and specification of the behavioral interaction mechanisms that comprise the modeling framework are also discussed. The model application is then provided. Finally, concluding remarks along with possible extensions of the research work are given.

2. Literature review

The literature reports numerous models that differ in their application scope, underlying theoretical approach, required effort for calibration and validation, and scalability. For example, applications of existing models include modeling

pedestrian movements in closed facilities (e.g., transit terminals, worship facilities, museums and exhibit halls, etc.) as well as studying crowd dynamics in open areas (e.g., city centers, stadium zones and street carnivals). The applications range from capacity planning and level of service evaluation to emergency preparedness and evacuation studies. Different theoretical approaches have been adopted for these models. These approaches could generally be grouped into two classes: static and dynamic. Static models have typically used space syntax and sketch-plan techniques which provide a high-level of analysis including determining potential conflict points, identifying dominant walking trajectories, estimating approximate volumes, and performing line of sight analysis (e.g., Ercolano et al., 1997). Dynamic models typically use simulation techniques to model pedestrians' interactions with each other and with the surrounding environment (e.g., Algadhi and Mahmassani, 1990, 1991; Blue and Adler, 1998, 1999, 2001; Teknomo et al., 2001; Haklay et al., 2001; Turner and Penn, 2002; Helbing et al., 2002, 2005; Holden and Cangelosi, 2003; Batty et al., 2003; Hoogendoorn and Bovy, 2004; Abdelghany et al., 2005, 2010, 2012; Robin et al., 2009; Zheng et al., 2009; Wagoum et al., 2012; Crociani et al., 2014; Wąs and Lubaś, 2014; Van Toll et al., 2015). These models adopt different modeling approaches to represent the pedestrians' behavior including destination and route choice, adjustment of walking trajectory, walking speed, congestion aversion, and collision avoidance. They also include, for example, cellular automata models, lattice gas models, social force models, agent-based models, and fluid-dynamic models (Harney, 2002; Ronald, 2007; Castle et al., 2011; Duives et al., 2013). Examples of these models are given below.

As mentioned above, in this proposed model, a hybrid (two-layer or bi-resolution) network representation of the crowd facility is considered, where one layer consists of a high resolution Cellular Automata (CA) system. Blue and Adler (1998, 1999, 2001) are among the first to present a cellular automata simulation-based model to study pedestrian movement. Following this approach, the studied space is divided into symmetric cells such that one cell could be occupied by one pedestrian at any time. A pedestrian can move to an adjacent cell along their walking path only if this adjacent cell is not occupied by another pedestrian. The number of cells that can be occupied by a pedestrian in any simulation interval is a function her/his desired speed. Numerous extensions and applications of the basic cellular automata model have been reported in the literature over the past decade (Blue and Adler, 2001; Dijkstra et al., 2001; Burstedde et al., 2001; Schadschneider, 2001; Kirchner and Schadschneider, 2002, Kirchner et al., 2003, Weifeng et al., 2003, Abdelghany et al., 2005, Yamamoto et al., 2007, Yue et al., 2007, Sarmady et al., 2011, Zhang et al., 2012, Hsu and Chu, 2014; Li et al., 2015). For example, Kirchner and Schadschneider (2002) proposed a bionics-inspired cellular automata model to model pedestrians' herding behavior during evacuation. Kirchner et al. (2003) proposed a stochastic cellular automata model to represent friction effects and clogging during evacuation applications. Abdelghany et al. (2005) presented an enhanced model to represent the pedestrians' congestion aversion behavior and possible destination and route update as a function of the congestion dynamics in the facility. The lattice gas models are viewed as another articulation of the cellular automata approach, where each pedestrian is modeled as an active particle that moves on a grid. Examples of models that adopt the lattice gas approach can be found in Helbing et al. (2003), Nagai et al. (2004), and Isobe et al. (2004).

Other major modeling framework for crowd simulation includes social force models and agent-based models. Helbing and Molnar (1995) introduced the social force model for crowd dynamics. The model assumes that the movement made by each pedestrian is the result of several force terms that measure the internal motivation of the individual to perform certain actions. Examples of these force terms are: (a) the pedestrian's acceleration to maintain his/her desired movement speed; (b) the attractiveness to activity location or to the final destination; and (c) the pedestrian's tendency to maintain a certain distance from other pedestrians and obstacles. The social force model has attracted great attention from researches. For example, Parisi and Dorso (2005) studied the facility evacuation problem using the social force model, which allows modeling the behavior of the evacuees assuming different levels of panic. Seyfried et al. (2006) presented a model that extends the social force model to simulate pedestrian movement dynamics and examine the resulting speed–density relationship considering different approaches for representing the interaction among pedestrians. Lin et al. (2006) presented an agent-based system based on the social force model and applied it to an evacuation scenario. Song et al. (2006) introduced a modified version of the social force model entitled multi-grid model. The study considered an evacuation scenario where pedestrians are evacuating a large room with only one door. The study analyzed the influences of interaction forces and drift on evacuation time. Guo and Huang (2011) presented simulation models which extend the social force model to consider the pedestrians' direction visual field. The results show that considering this modeling feature allows more realistic representation of pedestrians' route choice in evacuation scenarios.

Agent-based models are generally more computationally demanding as they enable modeling the heterogeneity in the pedestrian behavior. The complexity of the model depends on the set of rules that govern the movement of each agent (Kurose et al., 2001; Hoogendoorn et al., 2002; Bandini et al., 2006; Henein and White, 2006; Pan et al., 2007; Campanella et al., 2009; Izquierdo et al., 2009). For example, Kurose et al. (2001) and Hoogendoorn et al. (2002) presented a model in which pedestrians are assumed to choose their routes based on a set of local optimizations in order to account for the fact that pedestrians do not have complete knowledge of the system. The complexity of the model increases rapidly when many combinations of destinations and goals are incorporated. Abdelghany et al. (2005) and Bandini et al. (2006) allowed agents in their cellular automata models to adopt heterogeneous behavior in terms of desired speed, congestion aversion behavior, and willingness to update destination due to congestion. Izquierdo et al. (2009) presented an evacuation simulation model for estimating evacuation times, which is inspired by the so-called Particle Swarm Optimization (PSO). The PSO-based model allows for assessment of the behavioral patterns followed by individuals during a rapid evacuation event. Robin et al. (2009) developed an agent-based model in which each pedestrian chooses her route using a utility-based

discrete choice model. Pedestrians are assumed to evaluate the utility of the different route alternatives which describes their attractiveness in terms of several variable including the tendency of pedestrian to walk toward destination, avoid collisions, maintain desired speed, etc. The analogy between crowd movements and fluid dynamics has inspired the use of fluid dynamic models to represent crowd movement especially in high density situations (Algadhi and Mahmassani, 1990; AlGadhi and Mahmassani, 1991; Helbing et al., 2002). These models describe how density and velocity change over time and space using a set of partial differential equations. For example, Hughes (2000, 2002, 2003) derived continuum models to describe the motion of pedestrians as a two-dimensional fluid flow. Earlier, Algadhi and Mahmassani (1990) developed a bi-class, multi-directional continuum model of pilgrim movement in the Jamarat area of the Muslim pilgrimage in Saudi Arabia, including calibration of a bi-directional speed–density relation using actual observations (AlGadhi et al., 2002). The models were shown to capture observations of pedestrian behavior.

Several studies focus on pedestrian behavior analysis under different congestion levels. The main goal is to define the key parameters that affect pedestrian behavior and estimate the values of these parameters to be used in simulation models (Sarsam and Abdulameer, 2015; Wolinski et al., 2014; Karndacharuk et al., 2013; Rastogi et al., 2013; Moussaïd et al., 2010; Antonini et al., 2006; Hoogendoorn and Daamen, 2005). These behavior parameters are related to pedestrian speeds and speed fluctuations (Young, 1999; Ishaque and Noland, 2008; Chandra and Bharti, 2013; Brščić et al., 2014; Bandini et al., 2014a,b; Saberi et al., 2015; von Sivers and Köster, 2015), trajectory estimation and collision avoidance (Gao et al., 2014; Plaue et al., 2011; Johansson and Helbing, 2010; Gandhi and Trivedi, 2006), congestion aversion (Lachapelle and Wolfram, 2011), self-organizing (Helbing et al., 2001; Moussaïd et al., 2009), and pedestrian speed–flow–density relationships (Chattaraj et al., 2009). Recently, Gupta and Pundir (2015) presents an extensive review of literature for various existing studies on pedestrian flow characteristics under different traffic conditions and on different pedestrian facilities in urban areas. The review compares the values of various parameters of pedestrian movement that are of fundamental importance in any pedestrian modeling approach. The review highlights the lack of a global and detailed consideration of pedestrian behavior.

Several commercial software applications have been developed over the last two decades. Each application adopts one of the approaches described above as a basis for modeling the crowd behavior. An example of these applications is VISSIM which integrates pedestrian simulation and vehicle simulation in one software program (Fellendorf and Vortisch, 2010). The tool allows the user to define main routes between the origin–destination points. Pedestrians are assumed to update their walking trajectories along these paths to avoid congestion and obstacles following the social force model. The Urban Analytics Framework (UAF) software (Quadstone Paramics Website) also integrates both vehicular and pedestrian traffic. Its pedestrian simulation component is based on the pedestrian/crowd simulation algorithm, Myriad II Crowd Movement Algorithm, developed by Still (2000). The model adopts an agent-based approach which incorporates four intuitive behavioral rules, and one displacement rule. Each agent tries to reach its objective, while trying to reach its maximum desired speed. An agent must also maintain a minimal distance from other objects in its environment, while having a certain reaction time to the external events. The rule of displacement is based on the principle of the least effort, making it possible for the agent to choose the shortest route in terms of displacement time. Legion is an agent-based simulation model that employs a microscopic simulation approach based on the above-mentioned social force model. The model treats space as a continuum, using spatial objects (entrances, exits, escalators, etc.) to define space utilization (Legion Software website). The simulation navigates entities on the least-effort principle. Each pedestrian chooses its next step in an effort to find the best compromise between directness of path, speed and comfort. These decisions take into account an agent's preferences and objectives as well as the context, environment including avoiding other nearby pedestrians. The model is very sensitive to the values of its endogenous parameters. If it is not properly calibrated, the model could result in a situation of gridlock under moderate and high densities of conflicting traffic. A model for simulating large-scale crowds at interactive rates based on the principle of least effort (PLE) is developed by Sud et al. (2008). Daamen (2002) presents SimPed, which is a model for larger sale facilities such as train stations. However, the model does not treat scenarios of high densities. The highest density reported in the mode is about 2 persons/m^2. The approach uses an optimization method to compute a biomechanically energy-efficient, collision-free trajectory that minimizes the amount of effort for each heterogeneous agent in a large crowd. Application of the model in several test environments showed its ability to generate most observed phenomena such as lane formation and crowd compression at high congestion levels. The SimWalk software adopts a micro-simulation modeling approach where every single pedestrian is modeled individually with specific goals and behavior rules. The model captures both normal as well as panic behavior of pedestrians in complex environments. The approach integrates the social force model and a shortest-path algorithm to generate the pedestrians' walking trajectory. A recent application of the SimWalk to model the crowd movement in the core of the Holly Mosque in Mecca, the same application considered in this research, was limited to simulating 1000 agents as presented in Zainuddin et al. (2009). Such a small number of agents presents a significant simplification and is not expected to support actual system design and operational decisions.

Several of the above models, especially those commonly used in practice, undergo periodic enhancements as the body of application experience expands and user expectations of the models increase. Nonetheless, in their present form they share one or more of the following limitations. First, their ability to handle complex conflicting pedestrian movements tends to degrade as the density levels increase. Some of these models provide acceptable patterns of pedestrian flow dynamics under low densities of conflicting traffic. However, as the densities of conflicting traffic increase, possibly unrealistic patterns, including complete gridlock might emerge. The formation of these partial or complete gridlock instances result in unrealistic representation of the congestion phenomena and inaccurate estimates of the measures of performance. Second, most of

these models are computationally cumbersome especially for large-scale facilities with high demand levels. Thus, the extended running time limits their application to examine multiple design alternatives and crowd management schemes, which is usually needed in most real-world applications (Tunasar, 2013). Finally, some of these models have not undergone comprehensive calibration and validation studies, especially under high density levels. This is mainly due to the limited availability of field data, particularly at the disaggregate level, that can be used for calibration of the different behavior components of the model or for overall model validation.

3. Modeling framework

Notations

T	set of simulation intervals in the horizon, indexed by t
T'	set of loading intervals for pedestrian demand in the horizon, indexed by τ
N	set of nodes in the network model, indexed by n
M	set of links in the network model, indexed by m
O	set of origin (entrance) nodes $O \in N$, indexed by i
D	set of destination (exit) nodes $D \in N$, indexed by j
P	set of pedestrians in the facility, indexed by p
Q_{ij}	set of possible activity patterns for pedestrians entering the facility at node $i \in N$ and existing at node $j \in N$, indexed by q
C	set of cells in the cellular automata system, indexed by c
$C_n \in C$	set of cells representing node n, indexed by c_n
$C_m \in C$	set of cells representing link m, indexed by c_m
AC_c	set of adjacent cells to cell c
a	the area of the cell in the cellular automata system (m^2)
L_m	length of link $m \in M$ (m)
R_m	set of feasible walking trajectories along link $m \in M$, indexed by r_m
C_{r_m}	sequence of cells along walking trajectory r_m
AC_{r_m}	set of adjacent cells defining the vicinity of walking trajectory r_m
V_m^t	average walking speed along link $m \in M$ in time interval $t \in T$ (m/s)
K_m^t	pedestrians density along link $m \in M$ in time interval $t \in T$ (passengers/m^2)
tt_m^t	travel time of link $m \in M$ in time interval $t \in T$ (seconds or minutes)
δ_c^t	a binary variable to describe cell occupancy at time interval $t \in T$, which is equal to 1 if cell $c \in C$ is occupied at time t, and 0 otherwise
d_{ijq}^{τ}	number of pedestrians entering the facility at node $i \in I$ and existing at node $j \in I$ and follow activity pattern $q \in Q_{ij}$ in loading interval $\tau \in T'$
i_p	the entry node of pedestrian $p \in P$
j_p	the exit node of pedestrian $p \in P$
k_p	the route of pedestrian $p \in P$ which is defined in terms of a sequence of a sequence of links $M_k \in M$
v_p	desired (free-flow) walking speed for pedestrian $p \in P$ (m/s)
u_p	maximum congestion threshold accepted by pedestrian $p \in P$ along her movement trajectory (passengers/m^2)

Fig. 1 illustrates the overall modeling framework, which consists of four main modules: input, network builder, simulator and output. The input module processes the input data which includes: (a) geometrics of the facility and (b) demand loading pattern, planned activities, and behavioral characteristics. The geometrics description includes defining all spaces together with their shapes and dimensions, and illustrates how they are connected. It also provides the locations and dimensions of all gates and obstacles. This information is typically extracted from the facility's CAD files. The pedestrian demand input is in the form of a time-dependent origin–destination demand matrix. This matrix specifies the number of pedestrians entering and exiting the facility from the different gates in the different time intervals. In addition, the major activities expected in the facility and the percentage of pedestrians who follow these activities are assumed given. This demand data is used to specify the number of pedestrians d_{ijq}^{τ} generated at entrance gate $i \in I$ in demand loading interval $\tau \in T'$ and planning to exit the facility using exit $j \in J$ after completing chain of activities $q \in Q_{ij}$.

Next, for each pedestrian $p \in P$ the desired walking speed v_p is defined, which delineates the average distance a pedestrian can move per unit of time when allowed to walk freely in the area. In addition, the pedestrian's attitude toward congestion is defined by the congestion aversion threshold u_p. This threshold decides the maximum density that a pedestrian is willing to move through along her/his route. A low threshold indicates a congestion-averse pedestrian, who would rather detour around high congestion pockets. The desired speed and congestion aversion attributes are assigned randomly to the pedestrians following predefined input distributions that describe the population behavior. Moreover, the model allows the values of these attributes to change over time. Pedestrians are frequently observed to change their free-flow speed or congestion

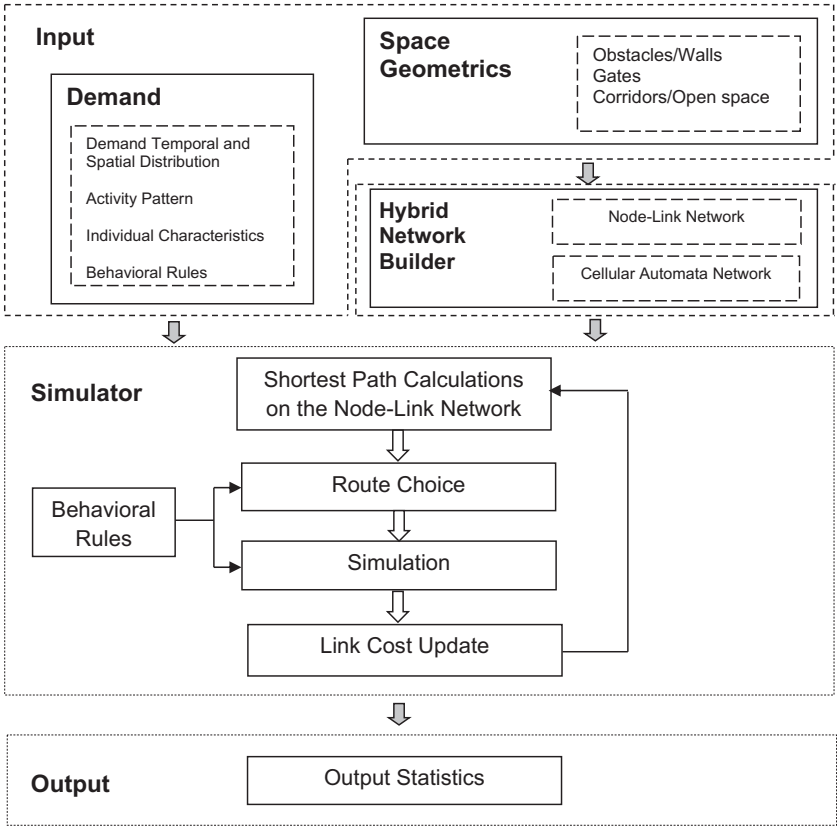

Fig. 1. Overall modeling framework.

perception threshold when they perform certain activities or when they get closer to their destinations. If data on such behavior is available, it is used to specify how pedestrians change their speeds and/or congestion aversion thresholds in different circumstances. In such case, the time index t is added to represent the time-varying desired speed v_p^t and congestion aversion u_p^t characteristics of each pedestrian.

Given the geometric features of the facility, a hybrid representation is used to model the facility, as illustrated in Fig. 2. The first layer (lower layer in Fig. 2) consists of a Cellular Automata (CA) system in which all open spaces are divided into a set of uniform cells C such that the size of each cell is to be occupied by one pedestrian (Blue and Adler, 1999, 2001; Dijkstra et al., 2001; Burstedde et al., 2001; Weifeng et al., 2003; Abdelghany et al., 2005; Yamamoto et al., 2007; Yue et al., 2007; Sarmady et al., 2011; Zhang et al., 2012; Hsu and Chu, 2014; Li et al., 2015). Each cell is defined by its location and set of adjacent cells AC_c. Two cells are defined to be adjacent if they share any of their boundaries. All cells that are occupied by obstacles are marked as inaccessible. The second layer (upper layer in Fig. 2) is a node–link network representation, which is defined using a set of nodes N and a set of links M, respectively. A node $n \in N$ represents main points along major paths in the facility. It could also represent a target point for an intermediate activity or a final destination. Each link $m \in M$ represents the line of sight of pedestrians standing at the upstream node of the link and heading to its downstream node. There will be no link connecting any two nodes that have an obstruction preventing reaching between them. Nodes and links in this layer are used to describe possible walking paths in the facility. Generally, as illustrated in more detail hereafter, having more nodes and links in network enhances the representation of moving trajectories for pedestrians in the facility. The converse is also true. The upper level layer is devoted to capturing the strategic behavior of the pedestrians as it is used to represent their destinations and the general paths used to reach these destinations. The lower level layer captures the tactical movements of the pedestrians. It describes the movement of each pedestrian as a sequence of cells occupied over time along her/his path to reach the destination.

The two layers are linked by associating each node $n \in N$ in the first layer with a set of cells $C_n \in C$ in the second layer. This set of cells is selected such that when a pedestrian chooses a node as a final or intermediate destination, reaching any of these cells is considered equivalent to arriving at the corresponding target node. Thus, each node is actually is in the form of a strip that includes a few cells. For example, if a node represents an exit gate, all nodes along this gate are set to be associated with this node. In the extreme case, as more nodes are added to the network model of the first layer, each node would be associated with one cell in the CA layer. Thus, the two layers used to represent the facility converge into one layer.

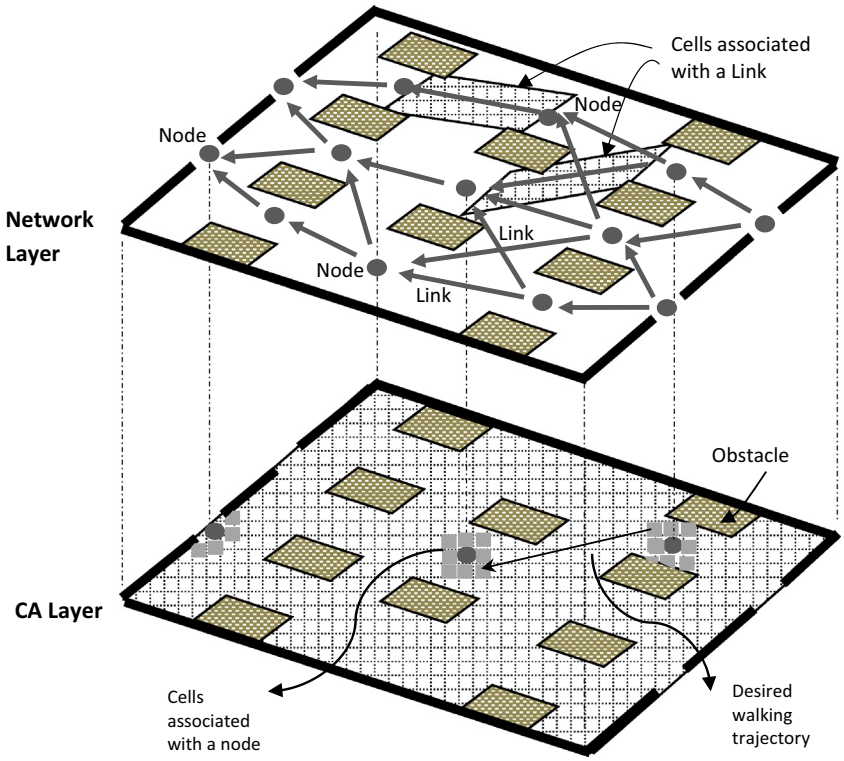

Fig. 2. Example of hybrid network representation.

Accordingly, any arc connecting any two cells on any two adjacent nodes represents a potential walking trajectory along the link that connects these two nodes. Each link $m \in M$ is associated with a set of cells $C_m \in C$, which covers the area representing the envelope of all possible walking trajectories along that link. This area is usually rectangular with its length is the length of the link and its width is the smallest of the average spacing between the nodes or a predefined value in the range of 2–3 m. Nodes (strips) are added to the network representation such that any arc connecting between any two cells on the strips can be part of a pedestrian trajectory. As more nodes are added, they improve the model resolution, as more possible trajectories are generated. Typically, there is a trade-off between the number of nodes in the network and the model computation requirements. Adding nodes every 2–3 m proved to provide realistic representation of most pedestrian trajectories. Accordingly, the area considered to determine the density around each link $m \in M$ is defined by the length of the link and a width of 2–3 m. The percentage of occupied cells in this area is used to describe the link's level of congestion, as described hereafter.

Pedestrians are generated according to their scheduled entry times. The set of activities that each pedestrian is planning to perform in the facility, together with their order and locations, is also given. The duration of the activity could be fixed and pre-defined, or system-dependent (e.g., waiting time in a queue to perform the activity). Each pedestrian $p \in P$ is loaded into the facility at his/her designated entry node i_p through an entry cell $c_{i_p} \in C_{i_p}$. The entry cell c_{i_p} is selected from the set of cells associated with the entry node $i_p \in N$ of this pedestrian. Each entry node $i \in N$ is associated with a virtual queue. If the facility is full and there are no empty cells by the time a new pedestrian is generated, this pedestrian is assumed to join the virtual queue (i.e., a queue outside the boundaries of the facility). Pedestrians are loaded from the entry queue into the facility following the first-in–first-out rule. Once a pedestrian is generated, this pedestrian is assigned a path k_p to her/his destination of her/his first activity. A path k_p is defined in terms of a set of subsequent links as shown in Fig. 3.

To model pedestrians' route choice behavior, a shortest path algorithm is periodically activated to determine the optimal set of paths from all nodes to all destinations. The activation cycle is selected such that it reflects the congestion dynamics in the facility. The implemented version of the algorithm is formulated to optimize a generalized cost measure that describes the pedestrians' walking impedance. In the current implementation, the link's travel time $tt_m^t = L_m/V_m^t$ is used to describe the pedestrians' walking impedance. Speed–density relationships have been proposed to determine the pedestrians' average walking speed as a function of the prevailing density (e.g., Fruin, 1971; Virkler and Elayadath, 1994; Lam and Cheung, 2000; AlGadhi et al., 2002; Chen et al., 2010). As shown in (1), the walking speed V_m^t along link m at time t is calculated as a function $f(\cdot)$ of the pedestrians density in the vicinity of the link K_m^t. The function $f(\cdot)$ is calibrated to represent the observed walking behavior and associated congestion dynamics in the facility. In the current implementation of the model, a linear function is assumed where the maximum speed is the pedestrian desired speed and the jam density is an estimated

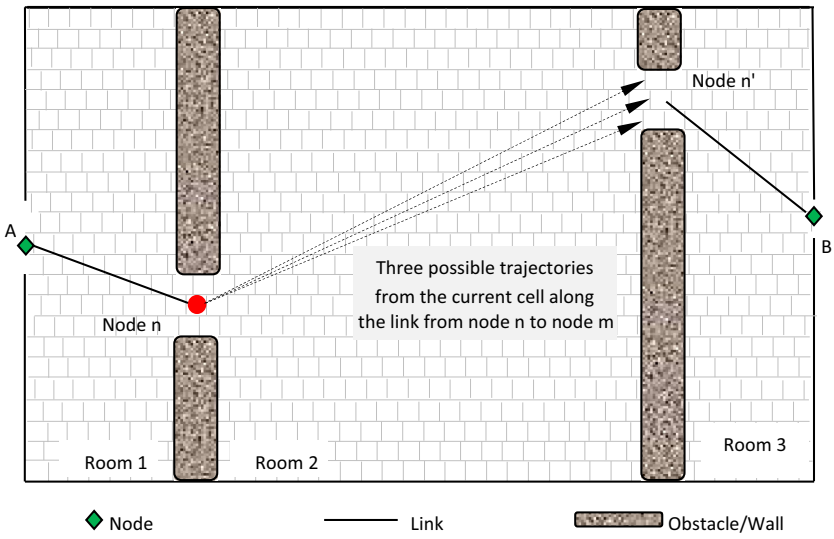

Fig. 3. Possible link trajectories.

parameter based on the observed congestion phenomenon in the facility (Older, 1968; Navin and Wheeler, 1969; Fruin, 1971; Sarkar and Janardhan, 2001; Tanaboriboon et al., 1986; Tanaboriboon and Guyano, 1991). Without loss of generality, any other relation form can be used. Given the set of cell $C_m \in C$ that defines link m, the density K_m^t is computed as the number of occupied cells in C_m at time t divided by the total area covered by all the cells in C_m, as illustrated in (2).

$$V_m^t = f(K_m^t) \tag{1}$$

$$K_m^t = \frac{\sum_{|C_m|} \delta_c^t}{|C_m| \cdot a} \tag{2}$$

In highly congested scenarios, when such behavior is observed, the model allows each pedestrian to periodically change her/his destination to avoid congestion, if the same activity can be conducted at the alternative destination. The assigned path could depend on the pedestrian's level of familiarity with the facility and access to real-time information on the level of congestion at the different parts of the facility, if any. In general, pedestrians familiar with the facility and those who have access to route guidance information are expected to use more efficient paths. The model's structure is ready to represent the behavior of unfamiliar pedestrians through, for example, assigning them to routes with some intended inefficiency. We focus our presentation on the case in which pedestrians are familiar with the facility and are able to plan efficient routes for their tours.

The simulation component captures the congestion dynamics resulting from the pedestrians' movement decisions in the area. It tracks the pedestrians' movements, while performing their planned activities until they exit the area. As mentioned above, each pedestrian $p \in P$ is assigned a route k_p that consists of a set of consecutive links $M_k \in M$. Pedestrians proceed from one link to the next along their paths. For each link $m \in M_k$, a walking trajectory $r_m \in R_m$ is selected by the pedestrian. The walking trajectory connects the pedestrian's current cell at the link's upstream node (strip) with a cell on the link's downstream node (strip). For example, in Fig. 3, for the pedestrian at node n and heading to node n' (i.e., link nn'), three possible walking trajectories are illustrated, which connect between the pedestrian's current cell at node n and three different cells at her/his next node n'. Pedestrians are assumed to select among these walking trajectories according to their congestion aversion behavior. For each feasible walking trajectory $r_m \in R_m$, the pedestrians' density $K_{r_m}^t$ along the vicinity of the walking trajectory AC_{r_m} is computed. These densities are then compared with the pedestrian's congestion aversion threshold u_p as illustrated in (3).

$$K_{r_m}^t = \frac{\sum_{|AC_{r_m}|} \delta_c^t}{|AC_{r_m}| \cdot a} \leqslant u_p \tag{3}$$

If multiple walking trajectories satisfy this threshold, the pedestrian is assumed to arbitrarily select one of them. Once a walking trajectory is identified, the pedestrian is assumed to proceed along the cells C_{r_m} of this walking trajectory. Given the pedestrian desired speed v_p, the number of steps that she/he can make in one simulation interval is determined. A step is a movement from a cell to the next adjacent cell along the selected walking trajectory. At every step, the density around the pedestrian's next cell is compared with her/his congestion aversion threshold. The set of adjacent cells AC_c is used to compute this density. A pedestrian can move to the next cell, only if this cell is not occupied by another pedestrian and the congestion aversion threshold of this pedestrian is satisfied. If the pedestrian fails to move into this cell, another adjacent cell

along the pedestrian's desired motion direction is attempted. If none of the adjacent cells are empty or satisfy the density condition, this pedestrian is assumed to remain in her/his current cell. Once the pedestrian reaches the downstream node of this link, the next link $m' \in M_k$ along her/his path is identified and the process continues until the pedestrian reaches her/his destination. If the current activity is completed, the pedestrian moves to the next destination in her/his activity plan. As the pedestrian completes all planned activities, she/he proceeds to the exit gate and no longer tracked in the system.

In highly congested conditions, having many pedestrians remain unmoved in their current location for a period of time can lead to sometimes unrealistic gridlock in the facility. Accordingly, a location swapping module is activated to allow the pedestrian to swap his/her cell with one of the pedestrians in the adjacent cell, given that they are both interested in their new cells (e.g., moving in opposite directions). The location of each pedestrian is consequently updated. This location swapping behavior is commonly observed in extremely congested situations. Adopting a rule to replicate this behavior allows the model to represent highly congested scenarios.

In order to provide an accurate evaluation of the performance of the facility, the framework is designed to generate a wide range of statistics and performance measures as part of its output. For example, for each pedestrian, the model produces her/his used trajectory, travel distance, travel time, and stopping time. The model also produces two indicators for the quality of pedestrian's walking experience. The first indicator is defined in terms of number of encountered conflicts along the pedestrian's path. A conflict is defined as the situation in which a pedestrian is unable to move to the next cell due to congestion, and a swapping maneuver with another pedestrian moving in a conflicting direction is performed. The second indicator measures the level of congestion around the pedestrian along her/his path. An area (e.g., circle with a pre-defined radius) is defined for each pedestrian. The percentage of occupied cells in this area is determined for each simulation interval. These statistics are aggregated for the entire facility to calculate average travel time, average stopping time, average density, and throughput. Furthermore, the model is equipped with animation capabilities that show each moving pedestrian as a particle. Colored particles are used to distinguish the pedestrians in terms of their relevant activities, characteristics, or surrounding conditions. For instances, simulated pedestrians could be color-coded based on their current activities such entering, exiting, circumambulation, etc. They can also be distinguished based on their personal characteristics such as free flow speed, stopping time in their current position, current speed, and congestion perception. They can also be distinguished based on their surrounding conditions such as level of density in their surrounding area and number of encountered conflicts.

4. Case study

4.1. The facility under consideration

The model is applied to study the crowd movement in the ground floor of Al-Haram Al-Sharif Mosque (Al-Haram) in the City of Mecca, Saudi Arabia during the pilgrimage (Hajj) season. Studying crowd dynamics in Al-Haram has been of interest of many researchers during the past two decades (Al-Haboubi and Selim, 1997; Abdelghany et al., 2005; Zainuddin et al., 2009; Curtis et al., 2011). Fig. 4a and b shows aerial photos of the Al-Haram complex, its main hall, and its surrounding open areas (piazzas) during the peak and off-peak periods. These pictures are taken before the recent undergoing expansion, which changed the shape and dimensions of its main hall and the surrounding buildings. Al-Haram mosque stands as a unique structure and place for processing huge numbers of people (millions) performing special rites instructed by the religion of Islam, resulting in a unique manifestation of crowd behavior. The resulting crowding levels pose enormous challenges in terms of enabling users to achieve the main objectives of their visit, as well as reliably providing the kinds of vital services expected at such large gatherings. Al-Haram consists of the main hall known as Al-Sahn (The Sahn), which is approximately 100 m by 130 m (Fig. 4c). The Sahn is surrounded by a multi-story building and another additional open area, with a total estimated capacity of 330,000 worshipers. At the center of the Sahn, a cube-shaped shrine building known as "Al-Ka'aba Al-Mosharafa" (The Ka'aba) is located. The Sahn and its direct surrounding areas are known as the Mataf system. The east side of the building is delineated by longitudinal building known as Al-Masa'a (The Masa'a). The Masa'a is a multi-story two-way corridor structure, which is visited as part of the rituals performed during Muslim pilgrimage in Mecca. On its ground floor, the corridor connects two small mountains known as Al-Safa on the south side and Al-Marwa on the north. The overall length of the Masa'a is about 390 m with a total width of 33 m. The width of the Masa'a is divided equally between the two walking directions. Each direction includes a small lane with separate right-of-way for mobility-impaired individuals with wheelchairs (Fig. 4d). Several openings are provided along the corridor to allow pedestrians to exit during an emergency. The estimated capacity of each floor of the Masa'a is about 50,000 pedestrians and the maximum density observed during the peak period is about 4–8 persons/m^2.

During the Hajj event, each of the nearly three million pilgrims has to visit the Mataf system, at least twice, to perform the "Tawaf" ritual. The Tawaf is a circumambulation process whereby pilgrims go around the Ka'aba a total of seven times in the counter-clockwise direction, starting from a predefined radial line known as the Mataf starting line. During circumambulation, each pilgrim tries to come closer to the Ka'aba, in the hope of reaching and touching it, and also to avoid circumambulation in larger-radius loops. Upon finishing the Tawaf, pilgrims try to find a way out of the Mataf system, causing notorious crowd conflicts with other entering and looping pilgrims. Depending on the rituals performed, pilgrims may need to proceed to the Masa'a after finishing the circumambulation. Each pilgrim has to walk between Al-Safa and Al-Marwa for seven times, in a ritual known as Al-Sa'iy (the Sa'iy).

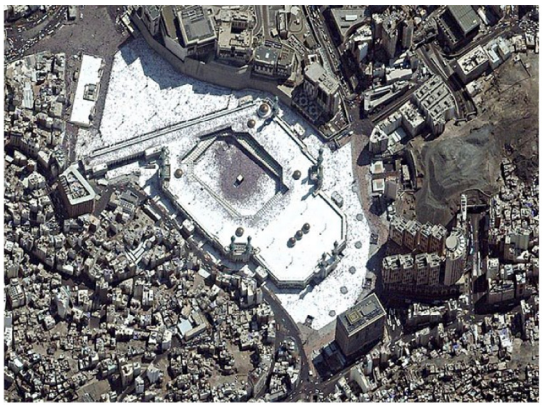

(a) Top view of the Haram at low demand levels

(b) Top view of the Haram at peak demand levels

(c) Al-Sahn area

(d) The Masa'a

Fig. 4. Snapshots of the Haram complex. *Source:* The Center of Research Excellence in Hajj and Omrah and the Custodian of the Two Holy Mosques Institute of Hajj Research at Umm Al-Qura University in Makkah, Saudi Arabi.

4.2. Facility configuration in the model

As described earlier, following the two-layer structure, the Mataf area is represented using a network layer and a CA layer. A special treatment is required while configuring these two layers to properly capture the circular movement of the pilgrims. As illustrated in Fig. 5a, the network model for the Mataf area is developed by first defining a series of radial hypothetical lines such that each line emanates along a radius from the center of the Ka'aba. These lines are drawn at equal angles (about 20–30°). Nodes are then inserted along each radial line with an average spacing of about 2.0 m. Links are connected between nodes along each of two consecutive radial lines. They represent the pedestrians' circular movement around the Ka'aba. Also, a radial-based CA system is developed as shown in Fig. 5b. The area is divided into equal rings. Each of these rings is then divided into equal cells. Each cell is of semi-square shape and of size that can be occupied by only one pedestrian. For the purpose of the study and to represent the severe congestion scenarios that are usually observed in these locations, an average cell dimension of 0.36 m is considered. The cell dimension is selected based on interviews with the facility operators who advised that a maximum density of about 7–8 pedestrians/m^2 is usually observed during peak operation hours. Other studies considered different number of cells per square meter ranging from 4 to 10 (Davidich and Köster, 2012; Leng et al., 2015). For each cell in the area, the set of adjacent cells is determined, usually to consist of (1) the set of inner adjacent cells located at the inner ring toward the Ka'aba, (2) the set of outer adjacent cells located at the outer ring toward the entrance/exit gates and (3) the adjacent cells in the same ring of the cell.

Pilgrims are loaded into the area following a predefined demand-loading pattern from any cell on the different entrance gates (origins). Upon entrance, the goal of each pilgrim is to approach the starting line and to be as close as possible to the Ka'aba. A node on the starting line is marked as her/his current destination. The shortest travel time path between the entry origin and the selected destination is determined. As mentioned earlier, this shortest path avoids obstacles and congested

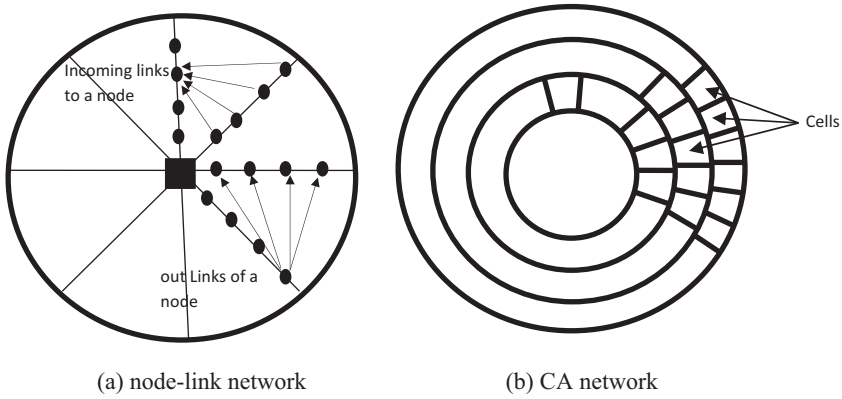

Fig. 5. The network layer and the cellular automata layer of the Mataf area.

spots along the pedestrian's route. The next node along the shortest path is identified and a target cell on this node is defined. The target cell is selected to define the walking trajectory on the current link given by the shortest path. Based on the selected movement trajectory, the next cell along this trajectory is selected from the set of adjacent cells.

Once a pilgrim reaches the start line of the Mataf, she/he starts to make seven loops around the Ka'aba. Each loop goes in the counter-clockwise direction, and ends at the same line. During circumambulation, each pilgrim tries to get closer to the Ka'aba shrine. She/he would also try to avoid looping at large-radius loops. Thus, the pedestrian selects a node on the next hypothetical radial line that best satisfies her/his goal. The pilgrim continues moving from one node to the next along the consecutive radial lines until she/he returns back to the Mataf starting line, completing one loop around the Ka'aba. The process of the Tawaf continues until all the seven loops are completed. Upon completing the Tawaf rituals, each pilgrim is assumed to find her/his way out of the Mataf system, seeking a less congested breath-taking zone outside the largest Tawaf circle. Accordingly, each pilgrim selects a destination outside the Mataf system and proceeds to this destination for contemplation, prayers and breath-taking. Next, pilgrims proceed to the Masa'a to perform the Sa'iy ritual. As mentioned above, during the Sa'iy, each pilgrim has to walk between Al-Safa and Al-Marwa marks for seven times. Therefore, pilgrims first walk from the Mataf system to the west side of the Masa'a and then they proceed to the south-side of the Masa'a (Al-Safa). The Sa'iy starts at Al-Safa by heading north to Al-Marwa along the right-hand side of the Masa'a corridor. Once the pilgrim reaches Al-Marwa, she/he turns back in the left-hand side corridor and heads south to Al-Safa. The process continues till all seven trips are completed. Upon finishing this ritual, pilgrims either exit the mosque or find a less congested area for breath-taking or contemplation. Fig. 6 shows several snapshots of the model replicating crowd movements filling the ground floor of Al-Haram. The blue-colored dots represent pilgrims entering the facility. The yellow[3] dots represent pilgrims approaching the Mataf, but who have not yet reached the Mataf starting line. The green dots represent pilgrims performing the seven loops of Tawaf. Finally, the red-colored dots represent pilgrims exiting the Mataf and heading to the Mas'aa corridor. The dark green dots represent pilgrims who are performing the Sa'iy ritual. It worth mentioning that the running time of the model varies by the loading scenario and how many individuals in the system at the same time. It runs on a computer with a processor Intel® Core™ i7-4900MQ CPU @ 2.80 GHz and Memory 32.0 GB in about 6–10 h.

As mentioned above, the model produces several visual-based measures of performance to assist the analyst in understanding the congestion dynamics in the facility and identifying spots with safety concerns. The three snapshots presented in Fig. 7 illustrate these measures of performance used to describe congestion level in the Sahn. They represent the state of the system at one time instance. Fig. 7a illustrates the spatial distribution of the density in the facility. Table 1 gives the coding colors used to represent the different density levels, together with the associated level of service. As shown in the figure, high spots of density occur near walls when pilgrims are pushing their way to complete the Tawaf. Also, other spots of high density are observed due to the conflict between exiting pilgrims and pilgrims continuing their Tawaf rituals. Finally, density tends to be higher near the Ka'aba than in the outer areas.

Fig. 7b shows the stopping time distribution. The green dots represent areas where pedestrians are experiencing no stopping because of congestion. The yellow dots represent areas where pedestrians stop at their current cells for less than 2 s, while the red dots represent areas where pedestrians stop for more than 2 s. Finally, Fig. 7c gives the distribution of the conflicts in the area. The red dots represent the case when a conflict is encountered. As mentioned above, a conflict is recorded when all the adjacent cells of the pedestrian are full and his location cannot be updated. One can observe the spatial correlation between these snapshots. Stopping time and conflicts are observed in areas of high density, which is observed near the northern and southern walls. The same pattern is also observed in the area where exiting pedestrians and heading toward the Mas'aa corridor are conflicting with those who are still performing the Tawaf rituals.

[3] For interpretation of color in Figs. 6 and 7, the reader is referred to the web version of this article.

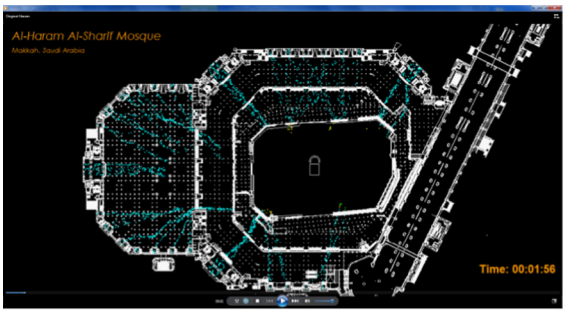

Snapshot 1 - Approaching the Mataf starting line from the entrance gates

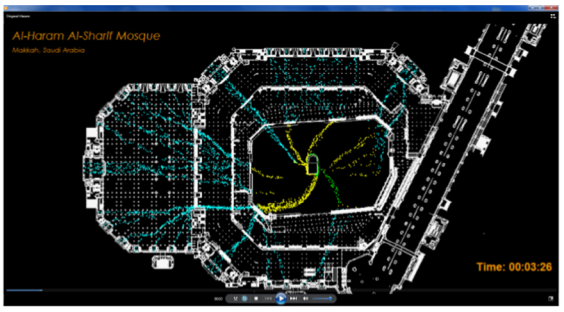

Snapshot 2 - Starting circumambulation

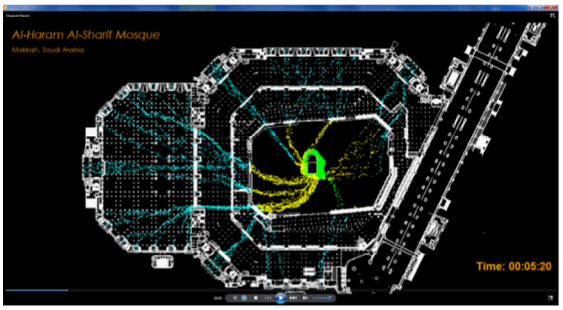

Snapshot 3 - Initial filling of Al-Sahn

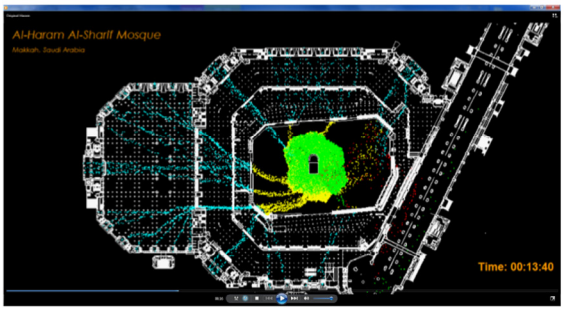

Snapshot 4 - Continue filling of Al-Sahn and pilgrims exit to the Masa'a corridor

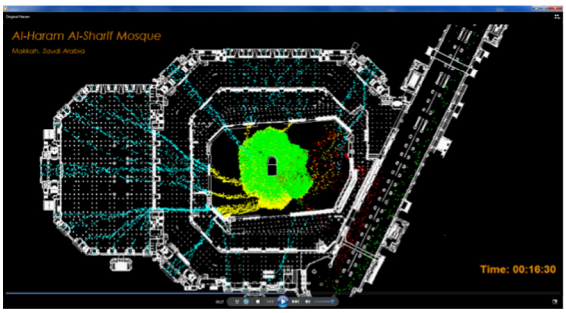

Snapshot 5 - Al-Sahn is almost full and more pilgrims area heading to the Masa'a corridor

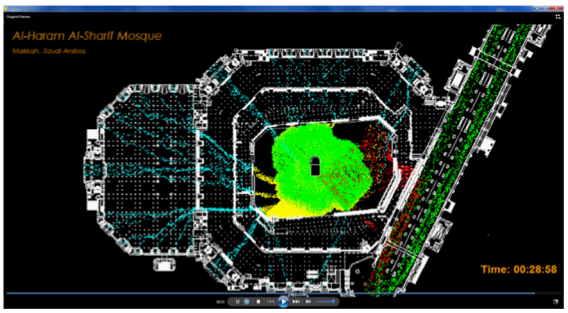

Snapshot 6 - The outer circle of Al-Sahn is completely full and the Masa'a is filling up

Fig. 6. Several snapshots of the model illustrating filling phenomena of the ground floor (Al-Sahn) of Al-Haram Al-Sharif Mosque in the City of Mecca, Saudi Arabia.

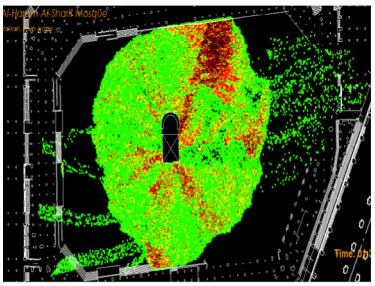

(a) Density

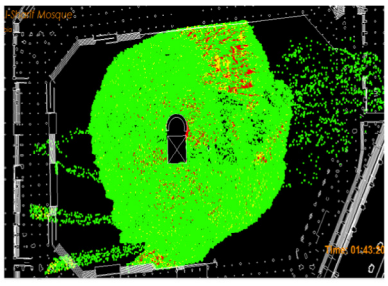

(b) Stopping time

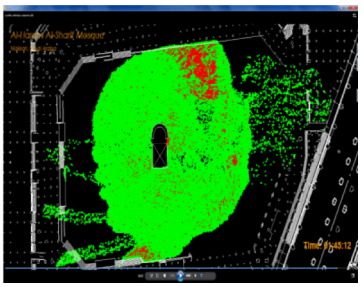

(c) Movement conflict

Fig. 7. Snapshots of Al-Sahn area illustrating the spatial distribution of the density, stopping time, and movement conflict.

Table 1
Color codes for the different density levels with the associated density levels.

Color code	Density level (pedestrian/m^2)	Level of service
Green	<2.5	LOS C or better
Yellow	2.5–4	LOS D
Red	4–6	LOS E
Brown	>6	LOS F

Table 2
Distribution of free flow speed.

Free flow speed	Percentage of the traffic
1 cell/s (0.36 m/s)	20
2 cells/s (0.72 m/s)	40
3 cells/s (1.08 m/s)	40

Table 3
Distribution of the congestion aversion threshold around the Ka'aba.

Location (radius in meter around the Ka'aba)	Congestion aversion threshold (pedestrians/m^2)
0–5	8.0
5–10	7.2
10–15	6.8
15–20	6.4
20–25	6.0
25–30	5.6
30–35	5.2
35–40	4.8
Elsewhere	4.0

4.3. Calibration of essential parameters

Calibration was performed to determine the distribution of essential parameters of the model including the free flow speed and the congestion aversion parameters for the pilgrims. For this purpose, four video recording were provided. These videos are recorded from cameras that are mounted along the structure that surrounds the circumambulation (Tawaf) area. The recording is available for 24 h. However, the free flow speed data is extracted in an off peak period of about 2 h. The congestion perception is collected during peak hours, when the circular area around the Ka'aba was completely full.

The free flow speed is measured by tracking a sample (about 1000 pedestrians) of individual pedestrians in the facility and measure their speed. Typically, free-flow speed is measured by tracking the time in which a pedestrian cross a predefined length under no surrounding congestion. Table 2 provides the distribution of the free flow speed used in the model. This distribution is obtained by a simple cluster analysis. As shown in the table, the population is divided into three speed categories. It is estimated that 20% of the traffic has a free-flow speed of 0.36 m/s, 40% has a free-flow speed of 0.72 m/s, and the remaining 40% has a free-flow speed of 1.08 m/s. The extracted video data is found relatively comparable to those collected in previous studies in similar context including Knoblauch et al. (1996), Koshak and Fouda (2008), Johansson et al. (2008), Li et al. (2012), and Yaseen et al. (2013). The speed represents the different classes of pilgrims including the elderly and female pilgrims who usually move at lower speeds. They also represent the nature of the facility where most pilgrims do not prefer to rush their rituals. As mentioned above, the actual speed is estimated as a function of the level of congestion (density) along each link. For this purpose, a linear speed–density relationship is considered for all links in the facility, where a complete stop occurs at about 8.0 persons/m^2 and maximum speed of about 1.0 m/s occurs at zero density. Similarly, for each pedestrian in the sample, the average densities are tracked to measure pedestrian congestion aversion with respect to the density in the system. Table 3 gives the distribution of the congestion aversion threshold in 5-m radius away from the Ka'aba shrine. The values in the table match the observed behavior in Al-Sahn area where pilgrims tend to follow less congestion aversion behavior as they get closer to the Ka'aba. The congestion aversion threshold is given to be 8 persons/m^2 within 5 m from the Ka'aba and decreases to about 4 persons/m^2 at 40 m away from the Ka'aba.

5. Simulation results

The results of using the model to simulate the crowd dynamics in the facility are presented in this section. The goal is to examine the capability of the presented model in capturing the observed congestion pattern. Two main results are discussed.

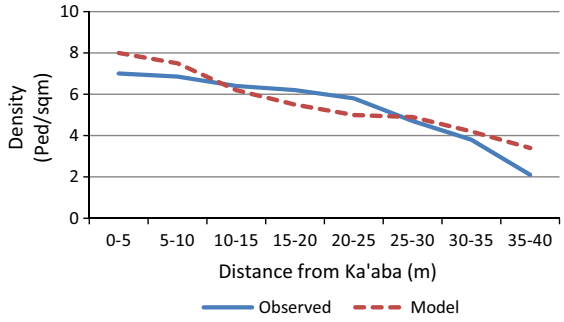

Fig. 8. The pedestrian density at different distances from the Ka'aba.

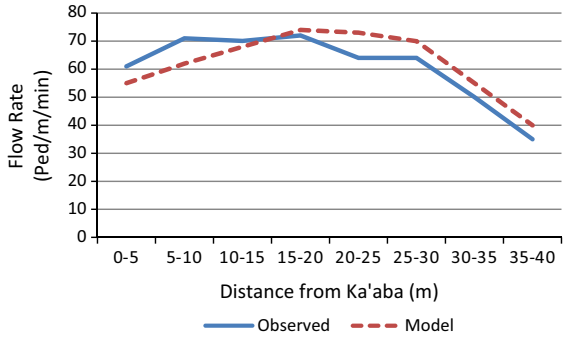

Fig. 9. The pedestrian flow rate at different distances from the Ka'aba.

The first result is related to illustrating the model capability in accurately representing the pedestrian density and flow pattern in the Sahn. The second result illustrates the use of the model to estimate the throughput of the Sahn. The average density and throughput around the Ka'aba are provided directly through the Center of Research Excellence in Hajj and Omrah and the Custodian of the Two Holy Mosques Institute of Hajj Research at Umm Al-Qura University in Makkah, Saudi Arabia, which regularly collect and analyze data about the facility.

Figs. 8 and 9 show the results related to estimating the average density and the flow rate at different distances from the Ka'aba, respectively. The results are recorded when the system reaches the steady state conditions. In other words, the results are recorded when the Sahn is full and the pedestrians' exit rate stabilizes. In both cases, the model's results are compared with the corresponding real-world measurements. As shown in these two figures, the model is able to replicate density and flow rate measures with acceptable accuracy. It captures the observed decrease in the density levels as the distance from the Ka'aba increases. It also captures the general pattern of the flow rate. The high density close to the Ka'aba makes the movement extremely difficult, which is translated in a low flow rate of about 50 pedestrians/m/s. As the distance from the Ka'aba increases, the congestion relatively eases and the flow rate gradually increases. At further distances, the flow rate decreases due to the decrease in the density. It should be noted that the validation effort presented here is an example of using available data to investigate how the model results reasonably match the observed phenomena. Similar to other microscopic models, performing a comprehensive model calibration and validation will be always encountered by constraints related to a) the quality of the data and its suitability to the calibration and validation exercise; and b) the time and cost budget available to perform the calibration and validation efforts. For example, the model has to be tested under different scenarios including different demand levels and different temporal and spatial loading distributions. The model should also be validated considering multiple facilities with different sizes and geometric layouts. Moreover, the model should be examined to make sure it captures the observed phenomena at disaggregate and aggregate levels. The model has to be validated at both the aggregate and the disaggregate levels. Of course, this comprehensive validation would require extensive data collection covering the entire facility. Collecting such data could be achievable for small facilities and during low demand level situations. The process becomes expensive and sometimes technically impossible for large and extremely crowded facilities such as the one considered in this paper.

The next set of results illustrates the use of the model to estimate the throughput of the Sahn in the steady state conditions. The throughput is measured in terms of number of pilgrims who completed their circumambulation rituals and proceeded to the corridor area. Based on field observations, a throughput of about 30,000 pilgrims/h is recorded in the peak period. Based on the results of several preliminary simulation results, the estimated throughput is found to be sensitive to the temporal demand loading pattern. For example, when a constant high demand loading rate is used to fill the Mataf,

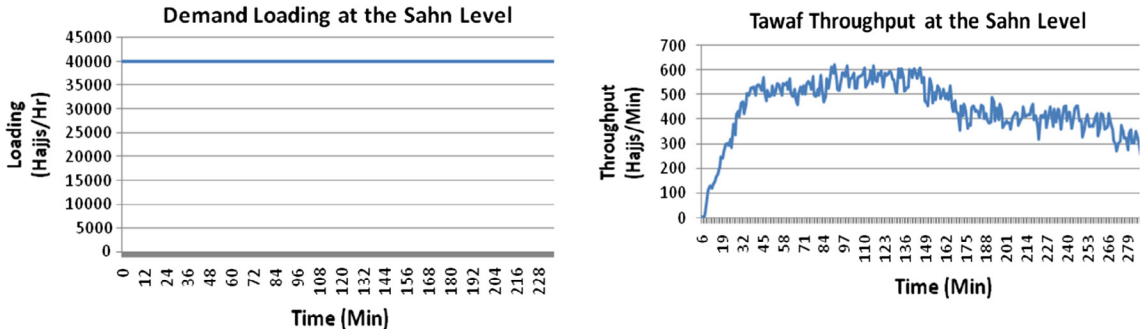

(a) Fixed Demand Loading Pattern at 40,000 pilgrims/hour

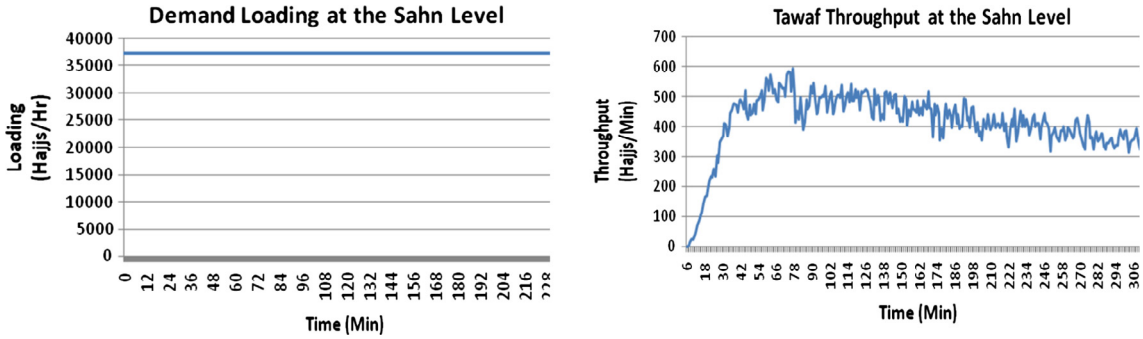

(b) Fixed Demand Loading Pattern at 37,500 pilgrims/hour

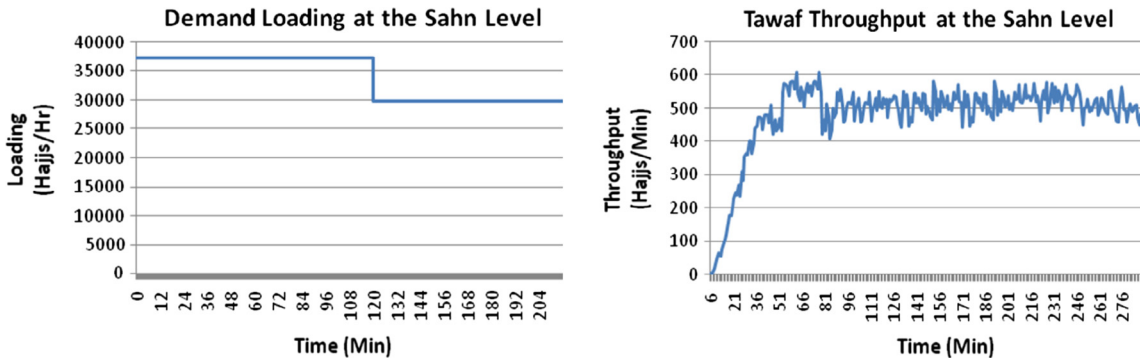

(c) Variable Demand Loading Pattern (37,500 and 30,000 pilgrims/hour)

Fig. 10. The throughput of Al-Sahn area considering different demand loading scenarios.

the maximum throughput of the Sahn could not be sustained as severe congestion builds up. Fig. 10 shows the estimated throughput as a function of the demand loading pattern. In Fig. 10a, a continuous loading rate of 40,000 pilgrims/h is used. The results show that while relatively high throughput values were initially obtained, these values could not be sustained for longer periods. A similar pattern is observed when the loading rate is reduced to 37,500 pilgrims/h as illustrated in Fig. 10b. A careful examination of these runs shows that spots of high density and low speed are quickly building near the Ka'aba as well as severe congestion along the perimeter of the Sahn. These congested spots as well as the congestion along the perimeters contributes to the reduction in the throughput. In Fig. 10c, a demand loading pattern is proposed where an initial loading of 37,500 pilgrims/h was used for 2 h followed by a rate of 30,000 pilgrims/h for another 2 h. As illustrated in the figure, a sustained throughput of about 530–540 pedestrian/min (31,800–32,400 pilgrims/h) was achieved, which is comparable to the observed throughput value (32,400 pilgrims/h). These scenarios are considered because it is the main concern of the operator is to estimate the system throughput under different demand loading scenarios. Typically, operators can control the entrance gates and accordingly the demand loading rate. This experiment show that after loading enough to fill the facility, the demand has to be reduced to prevent density from increasing. Increasing density is likely to reduce flow, speed, and throughput.

6. Conclusion

The paper presents a modeling framework for studying crowd dynamics in large-scale facilities. The framework judiciously manages the trade-off between ability to accurately capture congestion phenomena resulting from the pedestrians' collective behavior and scalability to model large facilities. It integrates a dynamic simulation-assignment logic with a hybrid (two-layer) representation of the facility. The top layer consists of a network representation of the facility, which enables modeling the pedestrians' route planning decisions while performing their activities. The bottom layer consists of a high resolution Cellular Automata (CA) system for all open spaces, which enables modeling the pedestrians' local maneuvers and movement decisions at a high level of detail. The model is applied to simulate the crowd movement in the ground floor of Al-Haram Al-Sharif Mosque in the City of Mecca, Saudi Arabia during pilgrimage. The analysis illustrates the model's capability to accurately represent the observed congestion phenomena in the modeled facility. Several extensions are considered for this research effort. For example, the model framework is suitable to model a wide range of crowd management strategies that are based on advanced traveler information systems. Examining the effectiveness of information provision strategies on the pedestrians flow pattern and overall facility performance is under investigation. Furthermore, to further validate the model, it will be applied to examine crowd movements in other facilities such as transit and airport terminals, stadia, and exhibition halls. Such facilities are characterized by pedestrians' behavior and associated congestion patterns are different from the one studied in this paper. Also, measurements at the disaggregate levels such as trajectories will need to be validated. Furthermore, it will be interesting exercise to compare model results with other modeling techniques. For example, pedestrian trajectories calculated in the model can be compared with trajectories generated by floor field approaches, in which the actual trajectories are delegated to the combination of floor fields and pedestrian decision model encapsulating the least effort principle. In addition, using the model to recommend optimal evacuation schemes during extreme conditions is under investigation. Finally, the use of the modeling framework as a part of a real-time crowd management system during peak seasons is under study.

References

Abdelghany, A., Abdelghany, K., Mahmassani, H., Al-Gadhi, S., 2005. Microsimulation assignment model for multidirectional pedestrian movement in congested facilities. Transport. Res. Rec.: J. Transport. Res. Board 1939, 123–132.

Abdelghany, A., Abdelghany, K., Mahmassani, H., Al-Ahmadi, H., Alhalabi, W., 2010. Modeling the evacuation of large-scale crowded pedestrian facilities. Transport. Res. Rec.: J. Transport. Res. Board 2198, 152–160.

Abdelghany, A., Abdelghany, K., Mahmassani, H., Al-Zahrani, A., 2012. Dynamic simulation assignment model for pedestrian movements in crowded networks. Transport. Res. Rec.: J. Transport. Res. Board 2316, 95–105.

Algadhi, S.A., Mahmassani, H.S., 1990. Modelling crowd behavior and movement: application to Makkah pilgrimage. Transport. Traffic Theory 1990, 59–78.

AlGadhi, S.A., Mahmassani, H., 1991. Simulation of crowd behavior and movement: fundamental relations and application. Transport. Res. Rec. 1320 (1320), 260–268.

AlGadhi, S.A., Mahmassani, H.S., Herman, R., 2002. A speed–concentration relation for bi-directional crowd movements with strong interaction. Pedestrian Evac. Dynam., 3–20

Al-Haboubi, M.H., Selim, S.Z., 1997. A design to minimize congestion around the Ka'aba. Comput. Ind. Eng. 32 (2), 419–428.

Antonini, G., Bierlaire, M., Weber, M., 2006. Discrete choice models of pedestrian walking behavior. Transport. Res. Part B: Methodol. 40 (8), 667–687.

Batty, M., Desyllas, J., Duxbury, E., 2003. Safety in numbers? Modelling crowds and designing control for the Notting Hill Carnival. Urban Stud. 40 (8), 1573–1590.

Bandini, S., Federici, M.L., Manzoni, S., Vizzari, G., 2006. Towards a methodology for situated cellular agent based crowd simulations. In: Engineering Societies in the Agents World VI. Springer, Berlin Heidelberg, pp. 203–220.

Bandini, S., Crociani, L., & Vizzari, G., 2014. Heterogeneous Speed Profiles in Discrete Models for Pedestrian Simulation. arXiv:1401.8132.

Bandini, S., Mondini, M., Vizzari, G., 2014b. Modelling negative interactions among pedestrians in high density situations. Transport. Res. Part C: Emerg. Technol. 40, 251–270.

Blue, V., Adler, J., 1998. Emergent fundamental pedestrian flows from cellular automata microsimulation. Transport. Res. Rec.: J. Transport. Res. Board 1644, 29–36.

Blue, V., Adler, J., 1999. Cellular automata microsimulation of bidirectional pedestrian flows. Transport. Res. Rec.: J. Transport. Res. Board 1678, 135–141.

Blue, V.J., Adler, J.L., 2001. Cellular automata microsimulation for modeling bi-directional pedestrian alkways. Transport. Res. Part B: Methodol. 35 (3), 293–312.

Brščić, D., Zanlungo, F., Kanda, T., 2014. Density and velocity patterns during one year of pedestrian tracking. Transport. Res. Procedia 2, 77–86.

Burstedde, C., Klauck, K., Schadschneider, A., Zittartz, J., 2001. Simulation of pedestrian dynamics using a two-dimensional cellular automaton. Physica A 295 (3), 507–525.

Campanella, M., Hoogendoorn, S., Daamen, W., 2009. Effects of heterogeneity on self-organized pedestrian flows. Transport. Res. Rec.: J. Transport. Res. Board 2124, 148–156.

Castle, C.J.E., Waterson, N.P., Pellissier, E., Le Bail, S., 2011. A comparison of grid-based and continuous space pedestrian modelling software: analysis of two UK train stations. In: Pedestrian and Evacuation Dynamics. Springer, US, pp. 433–446.

Chandra, S., Bharti, A.K., 2013. Speed distribution curves for pedestrians during walking and crossing. Procedia-Soc. Behav. Sci. 104, 660–667.

Chattaraj, U., Seyfried, A., Chakroborty, P., 2009. Comparison of pedestrian fundamental diagram across cultures. Adv. Complex Syst. 12 (03), 393–405.

Chen, X., Ye, J., Jian, N., 2010. Relationships and characteristics of pedestrian traffic flow in confined passageways. Transport. Res. Rec.: J. Transport. Res. Board 2198, 32–40.

Curtis, S., Guy, S.J., Zafar, B., Manocha, D., 2011. Virtual Tawaf: a case study in simulating the behavior of dense, heterogeneous crowds. In: 2011 IEEE International Conference on Computer Vision Workshops (ICCV Workshops). IEEE, pp. 128–135 (November).

Crociani, L., Invernizzi, A., Vizzari, G., 2014. A hybrid agent architecture for enabling tactical level decisions in floor field approaches. Transport. Res. Procedia 2, 618–623.

Daamen, W., 2002. SimPed: a pedestrian simulation tool for large pedestrian areas. In: Conference Proceedings EuroSIW, June, pp. 24–26.

Davidich, M., Köster, G., 2012. Towards automatic and robust adjustment of human behavioral parameters in a pedestrian stream model to measured data. Saf. Sci. 50 (5), 1253–1260.

Dijkstra, J., Jessurun, J., Timmermans, H.J., 2001. A multi-agent cellular automata model of pedestrian movement. Pedestrian Evac. Dynam., 173–181

Duives, D.C., Daamen, W., Hoogendoorn, S.P., 2013. State-of-the-art crowd motion simulation models. Transport. Res. Part C: Emerg. Technol. 37, 193–209.

Ercolano, J., Olson, J., Spring, D., 1997. Sketch-plan method for estimating pedestrian traffic for central business districts and suburban growth corridors. Transport. Res. Rec.: J. Transport. Res. Board 1578, 38–47.
Fellendorf, M., Vortisch, P., 2010. Microscopic traffic flow simulator VISSIM. In: Fundamentals of Traffic Simulation. Springer, New York, pp. 63–93.
Fruin, J., 1971. Designing for pedestrians: A level-of-service concept. New York metropolitan association of urban designers and environmental planners. Highway Res. Rec., 355
Gandhi, T., Trivedi, M.M., 2006. Pedestrian collision avoidance systems: a survey of computer vision based recent studies. In: Intelligent Transportation Systems Conference, 2006. ITSC'06. IEEE. IEEE, pp. 976–981.
Gao, Y., Chen, T., Luh, P.B., Zhang, H., 2014. Experimental study on pedestrians' collision avoidance. In: 2014 11th World Congress on Intelligent Control and Automation (WCICA). IEEE, pp. 2659–2663 (June).
Guo, R.Y., Huang, H.J., 2011. Route choice in pedestrian evacuation: formulated using a potential field. J. Stat. Mech.: Theory Exp. 2011 (04), P04018.
Gupta, A., Pundir, N., 2015. Pedestrian flow characteristics studies: a review. Transp. Rev., 1–21 (ahead-of-print)
Haklay, M., O'Sullivan, D., Thurstain-Goodwin, M., Schelhorn, T., 2001. "So go downtown": simulating pedestrian movement in town centres. Environ. Plann. B 28 (3), 343–359.
Harney, D., 2002. Pedestrian modelling: current methods and future directions. Road Transp. Res. 11 (4), 38.
Helbing, D., Molnar, P., 1995. Social force model for pedestrian dynamics. Phys. Rev. E 51 (5), 4282.
Helbing, D., Farkas, I.J., Molnar, P., Vicsek, T., 2002. Simulation of pedestrian crowds in normal and evacuation situations. Pedestrian Evac. Dynam. 21 (2), 21–58.
Helbing, D., Isobe, M., Nagatani, T., Takimoto, K., 2003. Lattice gas simulation of experimentally studied evacuation dynamics. Phys. Rev. E 67 (6), 067101.
Helbing, D., Buzna, L., Johansson, A., Werner, T., 2005. Self-organized pedestrian crowd dynamics: experiments, simulations, and design solutions. Transport. Sci. 39 (1), 1–24.
Helbing, D., Molnar, P., Farkas, I.J., Bolay, K., 2001. Self-organizing pedestrian movement. Environ. Plann. B 28 (3), 361–384.
Henein, C.M., White, T., 2006. Information in crowds: the swarm information model. In: Cellular Automata. Springer, Berlin Heidelberg, pp. 703–706.
Holden, R., Cangelosi, A., 2003. Cellular automata models of human traffic. In: First Conference of the European Social Simulation Association, Groningen, Netherlands.
Hoogendoorn, S.P., Bovy, P.H., Daamen, W., 2002. Microscopic pedestrian wayfinding and dynamics modelling. Pedestrian Evac. Dynam. 123, 154.
Hoogendoorn, S.P., Bovy, P.H., 2004. Pedestrian route-choice and activity scheduling theory and models. Transport. Res. Part B: Methodol. 38 (2), 169–190.
Hoogendoorn, S.P., Daamen, W., 2005. Pedestrian behavior at bottlenecks. Transport. Sci. 39 (2), 147–159.
Hsu, J.J., Chu, J.C., 2014. Long-term congestion anticipation and aversion in pedestrian simulation using floor field cellular automata. Transport. Res. Part C: Emerg. Technol. 48, 195–211.
Hughes, R.L., 2000. The flow of large crowds of pedestrians. Math. Comput. Simul. 53 (4), 367–370.
Hughes, R.L., 2002. A continuum theory for the flow of pedestrians. Transport. Res. Part B: Methodol. 36 (6), 507–535.
Hughes, R.L., 2003. The flow of human crowds. Annu. Rev. Fluid Mech. 35 (1), 169–182.
Ishaque, M.M., Noland, R.B., 2008. Behavioural issues in pedestrian speed choice and street crossing behaviour: a review. Transp. Rev. 28 (1), 61–85.
Isobe, M., Helbing, D., Nagatani, T., 2004. Experiment, theory, and simulation of the evacuation of a room without visibility. Phys. Rev. E 69 (6), 066132.
Izquierdo, J., Montalvo, I., Pérez, R., Fuertes, V.S., 2009. Forecasting pedestrian evacuation times by using swarm intelligence. Physica A: Stat. Mech. Appl. 388 (7), 1213–1220.
Johansson, A., Helbing, D., Al-Abideen, H.Z., Al-Bosta, S., 2008. From crowd dynamics to crowd safety: a video-based analysis. Adv. Complex Syst. 11 (04), 497–527.
Johansson, A., Helbing, D., 2010. Analysis of empirical trajectory data of pedestrians. In: Pedestrian and Evacuation Dynamics 2008. Springer, Berlin Heidelberg, pp. 203–214.
Karndacharuk, A., Wilson, D., Dunn, R., 2013. Analysis of pedestrian performance in shared-space environments. Transport. Res. Rec.: J. Transport. Res. Board 2393, 1–11.
Kirchner, A., Schadschneider, A., 2002. Simulation of evacuation processes using a bionics-inspired cellular automaton model for pedestrian dynamics. Physica A 312 (1), 260–276.
Kirchner, A., Nishinari, K., Schadschneider, A., 2003. Friction effects and clogging in a cellular automaton model for pedestrian dynamics. Phys. Rev. E 67 (5), 056122.
Koshak, N., Fouda, A., 2008. Analyzing pedestrian movement in Mataf using GPS and GIS to support space redesign. In: The 9th International Conference on Design and Decision Support Systems in Architecture and Urban Planning (July).
Knoblauch, R., Pietrucha, M., Nitzburg, M., 1996. Field studies of pedestrian walking speed and start-up time. Transport. Res. Rec.: J. Transport. Res. Board 1538, 27–38.
Kurose, S., Borgers, A.W., Timmermans, H.J., 2001. Classifying pedestrian shopping behaviour according to implied heuristic choice rules. Environ. Plann. B 28 (3), 405–418.
Lachapelle, A., Wolfram, M.T., 2011. On a mean field game approach modeling congestion and aversion in pedestrian crowds. Transport. Res. Part B: Methodol. 45 (10), 1572–1589.
Lam, W.H., Cheung, C.Y., 2000. Pedestrian speed/flow relationships for walking facilities in Hong Kong. J. Transport. Eng. 126 (4), 343–349.
Legion Software Website, 2013. <http://www.legion.com> (accessed in September).
Leng, B., Wang, J., Xiong, Z., 2015. Pedestrian simulations in hexagonal cell local field model. Physica A 438, 532–543.
Li, J., Fu, S., He, H., Jia, H., Li, Y., Guo, Y., 2015. Simulating large-scale pedestrian movement using CA and event driven model: methodology and case study. Physica A: Stat. Mech. Appl. 437, 304–321.
Li, S., Sayed, T., Zaki, M., Mori, G., Stefanus, F., Khanloo, B., Saunier, N., 2012. Automated collection of pedestrian data through computer vision techniques. Transport. Res. Rec.: J. Transport. Res. Board 2299, 121–127.
Lin, Q., Ji, Q., Gong, S., 2006. A crowd evacuation system in emergency situation based on dynamics model. In: Interactive Technologies and Sociotechnical Systems. Springer, Berlin Heidelberg, pp. 269–280.
Moussaïd, M., Helbing, D., Garnier, S., Johansson, A., Combe, M., Theraulaz, G., 2009. Experimental study of the behavioural mechanisms underlying self-organization in human crowds. Proc. Roy. Soc. Lond. B: Biol. Sci. (rspb-2009)
Moussaïd, M., Perozo, N., Garnier, S., Helbing, D., Theraulaz, G., 2010. The walking behaviour of pedestrian social groups and its impact on crowd dynamics. PLoS ONE, e10047.
Nagai, R., Nagatani, T., Isobe, M., Adachi, T., 2004. Effect of exit configuration on evacuation of a room without visibility. Physica A 343, 712–724.
Navin, F.P., Wheeler, R.J., 1969. Pedestrian flow characteristics. Traffic Eng. Inst. Traffic Eng., 39
Older, S.J., 1968. Movement of pedestrians on footways in shopping streets. Traffic Eng. Control 10, 160–163.
Pan, X., Han, C.S., Dauber, K., Law, K.H., 2007. A multi-agent based framework for the simulation of human and social behaviors during emergency evacuations. AI Soc. 22 (2), 113–132.
Parisi, D.R., Dorso, C.O., 2005. Microscopic dynamics of pedestrian evacuation. Physica A 354, 606–618.
Plaue, M., Chen, M., Bärwolff, G., Schwandt, H., 2011. Trajectory extraction and density analysis of intersecting pedestrian flows from video recordings. In: Photogrammetric Image Analysis. Springer, Berlin Heidelberg, pp. 285–296.
Quadstone Paramics Website, 2013. <http://www.paramics-online.com> (accessed in September).
Rastogi, R., Ilango, T., Chandra, S., 2013. Pedestrian Flow Characteristics for Different Pedestrian Facilities and Situations. European Transport, 53.
Robin, T., Antonini, G., Bierlaire, M., Cruz, J., 2009. Specification, estimation and validation of a pedestrian walking behavior model. Transport. Res. Part B: Methodol. 43 (1), 36–56.

Ronald, N.A., 2007. Agent-based Approaches to Pedestrian Modelling. Doctoral Dissertation. The University of Melbourne.
Saberi, M., Aghabayk, K., Sobhani, A., 2015. Spatial fluctuations of pedestrian velocities in bidirectional streams: exploring the effects of self-organization. Physica A 434, 120–128.
Sarkar, A.K., Janardhan, K.S.V.S., 2001. Pedestrian flow characteristics at an intermodal transfer terminal in Calcutta. World Transp. Policy Pract. 7 (1), 32–38.
Sarmady, S., Haron, F., Mohd Salahudin, M.M., Talib, A.Z.H., 2007. Evaluation of existing software for simulating of crowd at Masjid Al-Haram. Jurnal Pengurusan Jabatan Wakaf Zakat & Haji 1 (1), 83–95.
Sarmady, S., Haron, F., Talib, A.Z., 2011. A cellular automata model for circular movements of pedestrians during Tawaf. Simul. Model. Pract. Theory 19 (3), 969–985.
Sarsam, S.I., Abdulameer, M.W., 2015. Assessment of pedestrian walking characteristics at Erbil CBD. Int. J. Transport. Eng. Traffic Syst. 1 (1), 1–10.
Schadschneider, A., 2001. Cellular Automaton Approach to Pedestrian Dynamics-Theory. arXiv:cond-mat/0112117.
Song, W., Xu, X., Wang, B.H., Ni, S., 2006. Simulation of evacuation processes using a multi-grid model for pedestrian dynamics. Physica A 363 (2), 492–500.
Seyfried, A., Steffen, B., Lippert, T., 2006. Basics of modelling the pedestrian flow. Physica A 368 (1), 232–238.
Sud, A., Andersen, E., Curtis, S., Lin, M., Manocha, D., 2008. Real-time path planning for virtual agents in dynamic environments. In: ACM SIGGRAPH 2008 Classes. ACM, p. 55.
Still, G.K., 2000. Crowd Dynamics. Doctoral Dissertation. University of Warwick.
Still, K., 2010. Crowd Disasters. <http://www.gkstill.com/CV/ExpertWitness/CrowdDisasters.html> (accessed September, 2015).
Tanaboriboon, Y., Hwa, S.S., Chor, C.H., 1986. Pedestrian characteristics study in Singapore. J. Transport. Eng. 112 (3), 229–235.
Tanaboriboon, Y., Guyano, J.A., 1991. Analysis of pedestrian movements in Bangkok. Transport. Res. Rec., 1294
Teknomo, K., Takeyama, Y., Inamura, H., 2001. Microscopic pedestrian simulation model to evaluate lane-like segregation of pedestrian crossing. In: Proceedings of Infrastructure Planning Conference, vol. 24, November.
Tunasar, C., 2013. Analytics driven master planning for Mecca: increasing the capacity while maintaining the spiritual context of HAJJ pilgrimage. In: Simulation Conference (WSC), 2013 Winter. IEEE, pp. 241–251 (December).
Turner, A., Penn, A., 2002. Encoding natural movement as an agent-based system: an investigation into human pedestrian behaviour in the built environment. Environ. Plann. B 29 (4), 473–490.
Van Toll, W., Jaklin, N., Geraerts, R., 2015. Towards believable crowds: A generic multi-level framework for agent navigation. In: The 20th Annual Conference of the Advanced School for Computing and Imaging, ASCI.OPEN, Eindhoven, Netherlands.
Virkler, M.R., Elayadath, S., 1994. Pedestrian Speed–Flow–Density Relationships (No. HS-042 012).
von Sivers, I., Köster, G., 2015. Dynamic stride length adaptation according to utility and personal space. Transport. Res. Part B: Methodol. 74, 104–117.
Wagoum, A.U., Seyfried, A., Holl, S., 2012. Modeling the dynamic route choice of pedestrians to assess the criticality of building evacuation. Adv. Complex Syst. 15 (07), 1250029.
Wąs, J., Lubaś, R., 2014. Towards realistic and effective agent-based models of crowd dynamics. Neurocomputing 146, 199–209.
Weifeng, F., Lizhong, Y., Weicheng, F., 2003. Simulation of bi-direction pedestrian movement using a cellular automata model. Physica A 321 (3), 633–640.
Wolinski, D., Guy, S.J., Olivier, A.H., Lin, M., Manocha, D., Pettré, J., 2014. Parameter estimation and comparative evaluation of crowd simulations. Comput. Graph. Forum 33 (2), 303–312 (May).
Yamamoto, K., Kokubo, S., Nishinari, K., 2007. Simulation for pedestrian dynamics by real-coded cellular automata (RCA). Physica A 379 (2), 654–660.
Yaseen, S., Al-Habaibeh, A., Su, D., Otham, F., 2013. Real-time crowd density mapping using a novel sensory fusion model of infrared and visual systems. Saf. Sci. 57, 313–325.
Young, S., 1999. Evaluation of pedestrian walking speeds in airport terminals. Transport. Res. Rec.: J. Transport. Res. Board 1674, 20–26.
Yue, H., Hao, H., Chen, X., Shao, C., 2007. Simulation of pedestrian flow on square lattice based on cellular automata model. Physica A 384 (2), 567–588.
Zainuddin, Z., Thinakaran, K., Abu-Sulyman, I.M., 2009. Simulating the circumambulation of the Ka'aba using SimWalk. Eur. J. Sci. Res. 38 (3), 454–464.
Zhang, P., Jian, X.X., Wong, S.C., Choi, K., 2012. Potential field cellular automata model for pedestrian flow. Phys. Rev. E 85 (2), 021119.
Zheng, X., Zhong, T., Liu, M., 2009. Modeling crowd evacuation of a building based on seven methodological approaches. Build. Environ. 44 (3), 437–445.